

Crystalline structures and frustration in a two-component Rydberg gas

PACS numbers: 05.30.Rt, 32.80.Ee, 37.10.Jk, 64.70.Rh

Emanuele Levi, Jiří Minář, Juan P. Garrahan and Igor Lesanovsky

School of Physics and Astronomy, University of Nottingham, Nottingham, NG7 2RD, United Kingdom

Abstract. We study the static behavior of a gas of atoms held in a one-dimensional lattice where two distinct electronically high-lying Rydberg states are simultaneously excited by laser light. We focus on a situation where interactions of van-der-Waals type take place only among atoms that are in the same Rydberg state. We analytically investigate at first the so-called classical limit of vanishing laser driving strength. We show that the system exhibits a surprisingly complex ground state structure with a sequence of compatible to incompatible transitions. The incompatibility between the species leads to mutual frustration, a feature which pertains also in the quantum regime. We perform an analytical and numerical investigation of these features and present an approximative description of the system in terms of a Rokhsar-Kivelson Hamiltonian which permits the analytical understanding of the frustration effects even beyond the classical limit.

1. Introduction

Atoms in highly excited states — so-called Rydberg atoms — interact via power-law potentials, which in conjunction with an external laser drive give rise to intricate many-body phenomena. Recent experiments with Rydberg gases have revealed that the dynamical behavior of these systems is of surprising variety. Examples are the emergence of bistable behavior [1, 2], the observation of correlated aggregation of excitations [3] and of coherent excitation transport [4, 5, 6]. Strong interactions also become manifest in the structure of the ground state of Rydberg ensembles. Several theoretical works have predicted and studied the formation and the melting of crystalline phases [7, 8, 9, 10, 11, 12, 13, 14, 15]. But only recently it was shown that these crystalline states can be actually accessed experimentally [16].

Currently there is a surge of interest in atomic systems in which multiple Rydberg states are excited. One of the main motivations is the presence of an exchange interaction between Rydberg states of different atoms that results in coherent transport dynamics [4, 5, 6], the non-local propagation of light [17] as well as a non-trivial collapse and revival dynamics [18, 19]. Interesting physics emerges also in the absence of exchange interactions. The main reason is that depending on the Rydberg states the interaction between two atoms can vary by one or more orders of magnitude [20, 21]. This feature is exploited for example in all-optical transistors for light pulses [22, 23].

In this work we explore the many-body ground states of an atomic lattice gas in which two Rydberg states — or species — are simultaneously excited. We focus on a situation where interactions are present only between atoms of the same species. This is reminiscent of the Potts model [24], for which however only few studies exist that consider interactions that extend beyond nearest neighbors [25, 26, 27, 28]. We show that the ground state of the two-species Rydberg lattice gas features a surprisingly complex structure with a series of compatible to incompatible transitions. In the compatible case the two species can occupy the lattice such that they can both minimize their interaction energy independently. In the incompatible case this is not possible and it leads to mutual frustration. We provide analytical expressions for the regions of stability of the (in)compatible phases in the classical regime, i.e. in the limit of vanishing laser driving strength. The quantum regime is studied numerically as well as analytically with the help of an approximate Hamiltonian of Rokhsar-Kivelson form. These considerations show how frustration persists also in the quantum regime.

2. Description of the system

We consider a one-dimensional gas of atoms trapped in a lattice of spacing a with a single atom per site. The relevant internal level structure of the atoms is shown in Fig. 1a. The ground state $|g\rangle$ is coupled to two Rydberg nS -states ($|s\rangle$ and $|w\rangle$) via two laser fields with Rabi frequencies Ω_α and detuning Δ_α ($\alpha = s, w$). The fundamental interaction between two such atoms is to leading order given by the dipole-dipole

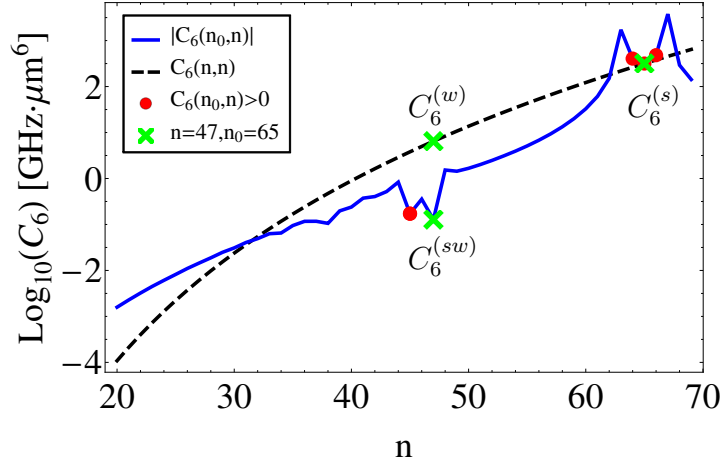


Figure 2. (Color online) Comparison of the van-der-Waals $C_6(n_0, n)$ coefficients describing the interaction strength between two rubidium atoms in Rydberg states with principal quantum number n_0 and n respectively. C_6 for the inter-species case is shown as a blue line (attractive interaction) and red circles (repulsive interaction). The black dashed line corresponds to the intra-species C_6 , i.e. $n_0 = n$. Green crosses represent a possible choice of Rydberg levels implementing the required hierarchy of interaction strengths assumed in our work. Identifying $n_0 = 65$ with the strong species and $n = 47$ with the weak one we get $C_6^{(s)}/C_6^{(w)} = 50.5$ and $C_6^{(w)}/C_6^{(sw)} = 49$, i.e. the hierarchy $C_6^{(s)} \gg C_6^{(w)} \gg C_6^{(sw)}$ is well respected (we have denoted here by $C_6^{(sw)} = C_6(65, 47)$ the inter-species C_6 coefficient).

as well as the frustration effects which we will discuss in the following.

3. Compatible to incompatible transition

We start by studying the case $\Omega_\alpha = \Delta_\alpha = 0$ in the thermodynamic limit, i.e. an infinite lattice, where Eq. (1) reduces to the Hamiltonian of a classical two-species Potts-model with (convex) $1/r^6$ interactions and inequivalent couplings ($V_s \neq V_w$). We are interested in finding the microscopic state which minimizes the interaction energy for given filling fractions of excitations ρ_s and ρ_w . For a single species and a general convex potential this problem was studied in [35, 29, 36, 37]. Given the filling fraction the convexity of the potential forces the system into the most homogeneous configuration achievable accounting for the lattice constraint, as shown by Hubbard in Ref. [29].

When two species are present it is in general not possible to minimize at the same time the interaction energy of both. An example is given in Fig. 1(b) for $\rho_s = 1/3$ and $\rho_w = 1/2$. Finding the actual ground state is simplified by our assumption $V_s \gg V_w$. Here, the configuration of the s -species can be considered as “frozen” and not

constrained by that of the w -species \ddagger . Atoms of the s -species will then arrange following the single species prescription of Ref. [29], that is calling r_l the distance between an s -atom and its l -th nearest neighbor, the s -atoms will be distributed on the chain with distances satisfying $r_l = \lfloor l/\rho_s \rfloor$ or $\lceil l/\rho_s \rceil$. This set of constraints identifies a unique distribution for the atoms of the s -species, and will in general lead to a deformed lattice formed by the remaining empty sites on which the minimum-energy arrangement of the atoms of the w -species needs to be found.

For the example shown in Fig. 1(b) the w -atom sitting in the doubly occupied site has to be moved to an empty site in a way that minimizes the increment in interaction energy. As shown in Fig. 1(c) the strong species leaves a distorted lattice with a density of empty sites given by $1 - \rho_s = 2/3$ and lattice spacings a and $2a$. The minimum interaction energy is then obtained by arranging the w -atoms according to the single species prescription of Ref. [29] considering that the filling fraction of the w species on the distorted lattice is $\rho_w/(1 - \rho_s) = 3/4$. This finally leads to the state depicted in Fig. 1(c). The mathematical proof of this method we provide in a separate publication, see Ref. [38]. Some examples of minimum interaction-energy configurations are shown in Fig. 1(d). From these considerations one finds that two cases, which depend on the filling fractions ρ_α , need to be distinguished: (i) The compatible case in which the two species assume their minimum-energy dispositions independently without interfering with each other. (ii) The incompatible case in which the strong species prevents the atoms of w -species from assuming their minimum energy configuration.

Understanding whether two filling fractions are compatible is generally a hard task which requires the study of the full arrangement of excitations. In the following analytical analysis we will consider filling fractions of the form $\rho_\alpha = 1/q_\alpha$, where both q_α are positive integers. Clearly, the minimum energy configuration is achieved when the α -atoms are arranged uniformly with distance q_α . The filling fractions are compatible only if they share a common divisor (see [38]). In the incompatible case the distribution of the w -atoms will be distorted and can be represented by repeated strings of repeated intervals of lengths $\dots q_w(q_w - 1)(q_w + 1)q_w \dots$, as shown for the example in Fig. 1(c).

Let us now turn to the discussion of the stability of the (in)compatible phases. So far we have assumed that the filling fractions ρ_α of the individual species are externally imposed. However, in practice the filling fraction is controlled by the parameters Δ_α in Hamiltonian (1) which act as chemical potentials [8, 14]. The question is then which state, or filling fraction, is actually stabilized in a given region of the $\Delta_s - \Delta_w$ manifold. As the distribution of the s -species is effectively independent from that of the w -atoms, we can study its stability with the single species method [36, 37, 14]. The stability of a given filling fraction ρ_w on the other hand is less simple to analyze, as it depends on the configuration of the s -atoms. We can obtain an analytical result for the transition to an incompatible state in the thermodynamic limit starting from a compatible arrangement

\ddagger This is strictly speaking true only in the asymptotic limit $V_s/V_w \rightarrow \infty$. Otherwise an additional assumption has to be made on the filling fractions, namely $V_s/V_w \gg 1$ and $\rho_s/\rho_w > 1$, the situation we consider here. See also [38] for details.

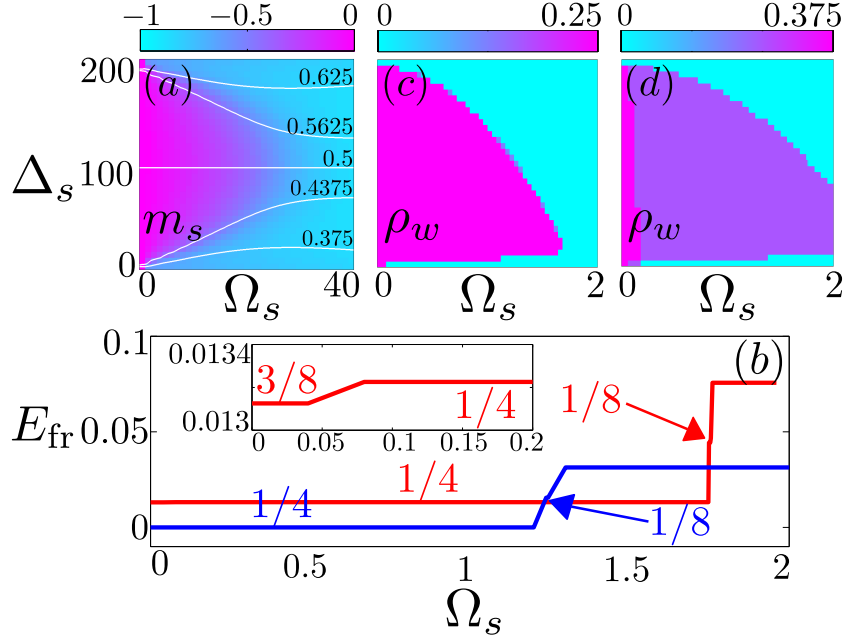


Figure 3. (Color online) Exact diagonalization results. (a) Density plot showing the transverse magnetization of the strong species m_s in a parameter regime Δ_s where the filling fraction in the classical limit ρ_s^{cl} , i.e. at $\Omega_s = 0$, is $1/2$. The white contours show lines of equal ρ_s . (b) Frustration energy (3) plotted along $\Delta_s = 102$, i.e. the $\rho_s = 1/2$ contour of (a). The blue and red lines correspond respectively to a compatible ($\rho_w^{cl} = 1/4$) and an incompatible ($\rho_w^{cl} = 3/8$) classical filling fraction. The value of ρ_w is indicated explicitly in the figure for some plateaus. The inset magnifies the first small jump in ρ_w in the incompatible cases. (c,d) Filling fractions of the weak species for compatible [$\rho_w^{cl} = 1/4$, (c)] and incompatible [$\rho_w^{cl} = 3/8$, (d)] case. The data were obtained with $V_s = 100V_w = 100$.

of atoms for which $\nu = q_w/q_s$ is integer (see Section 6 in [38]). The region of stability is delimited by

$$\frac{\Delta_w^{(\pm)}}{V_w} = \sum_{l=1}^{\infty} \left[\frac{1 \mp l(q_w - \nu)}{(lq_w)^6} \pm \frac{l(q_w - 2\nu)}{(lq_w \mp 1)^6} \pm \frac{l\nu}{(lq_w \mp 2)^6} \right]. \quad (2)$$

On the one hand a transition to an incompatible state takes place when $\Delta_w = \Delta_w^{(+)}$, the value of Δ_w for which the introduction of one more excitation is energetically favorable when keeping Δ_s fixed. In this case the distribution of the l -th nearest neighbor w -atoms which in the compatible phase is homogeneous, e.g. atoms at distance lq_w , is deformed by the introduction of $l\nu$ distances $q_w - 2$, and $l(q_w - 2\nu)$ distances $q_w - 1$. On the other hand there is a transition at $\Delta_w = \Delta_w^{(-)}$ at which the w species loses an excitation and the compatible distribution is deformed by the introduction of $l\nu$ distances $q_w + 2$, and $l(q_w - 2\nu)$ distances $q_w + 1$.

4. Quantum fluctuations and frustration energy.

We now address the question as to how quantum fluctuations introduced by a laser of finite driving strength affect the compatible to incompatible transitions and in particular the emergence of frustrated states. To this end we consider a non-zero value of Ω_s . This changes the state of the s -species from a classical one to a superposition of configurations with different excitation number. We are interested in how this impacts the classical arrangements of the w -species, i.e. at $\Omega_w = 0$. To quantify this we introduce the frustration energy

$$E_{\text{fr}} = E_{2\text{sp}}^{(w)}(\Delta_{s,w}; \Omega_s) - E_{1\text{sp}}^{(w)}(\Delta_w), \quad (3)$$

which measures by how much the strong species prevents the w -species from reaching its minimum energy configuration if it were alone. Here $E_{2\text{sp}}^{(w)}(\Delta_{s,w}; \Omega_s) = \langle H_w \rangle$, i.e. the expectation value of H_w [see Eq. (1)] and $E_{1\text{sp}}^{(w)}(\Delta_w)$ is the energy of the classical configuration of the w -species in the absence of s -atoms.

In the classical limit, $\Omega_\alpha = 0$, the frustration energy is zero when the detunings Δ_α are chosen such that they stabilize filling fractions ρ_α which are compatible. E_{fr} becomes in general larger with increasing Ω_s as increasing density fluctuations in the s -species force the w -atoms to assume configurations with increased energy. In order to study this behaviour in more detail we diagonalize Hamiltonian (1) for a chain of length $L = 8$ with periodic boundary conditions. This approach has the typical drawbacks of a small scale numerical study: the presence of finite size effects (though minimized by the periodic boundaries), and the fact that one is limited to filling fractions of the form p/L for $p \leq L$. We will see, however, that the results provide an intuitive understanding of the physics at work. Note furthermore, that the considered relatively small system size in fact comes close to what is currently realizable experimentally in the context of Rydberg atoms [39, 16].

For our numerical study we focus on a regime where the strong species in the classical limit forms a crystal with filling fraction $\rho_s^{\text{cl}} = 1/2$. With increasing Ω_s this crystal melts as is seen in Fig. 3(a) where we show a density plot of the transverse magnetization $m_s = (1/L) \sum_{k=1}^L \langle \sigma_k^{x(s)} \rangle$. The magnetization displays the typical lobe-structure [14], and the formation of a (longitudinally) paramagnetic state ($m_s = -1$) at large Ω_s . Here it is evident that the state of the strong species is formed by a superposition of states with different number of excitations.

Let us now have a look at the frustration energy when the weak species is added. The corresponding data is shown in Fig. 3(b). In the classical limit ($\Omega_s = 0$) we choose $\Delta_s = 102$ which corresponds to half filling of the strong species, $\rho_s^{\text{cl}} = 1/2$, and consider values of Δ_w which stabilize the compatible case $\rho_w^{\text{cl}} = 1/4$ ($\Delta_w \simeq 0.0159$ blue line) and the incompatible case $\rho_w^{\text{cl}} = 3/8$ ($\Delta_w \simeq 0.0314$, red line), respectively. We first determine the values of Δ_w numerically as the midpoints of the stability regions. In the compatible case one can use Eq. (2) to determine Δ_w . In the incompatible case on the other hand Eq. (2) cannot be applied directly. In the finite size case though, as previously mentioned, only fillings of the form p/L are accessible, and as such the

region of stability of $\rho_w^{\text{cl}} = 3/8$ extends from the upper boundary $\Delta_w^{(+)}$ for $\rho_w = 1/4$ to the lower boundary $\Delta_w^{(-)}$ for $\rho_w^{\text{cl}} = 1/2$. These cases are compatible such that we can use again Eq. (2) to estimate the midpoint of this region of stability. We find that the values obtained analytically from Eq. (2) are in remarkable agreement with the numerically determined values despite the small size of the system. At $\Omega_s = 0$, E_{fr} is zero for compatible densities and finite for incompatible ones. With increasing Ω_s , the w -species becomes more and more frustrated which is reflected in an increase of E_{fr} . Interestingly, this increase is step-wise and each step is accompanied by a change of the filling fraction ρ_w of w -atoms, whose value is provided in Fig. 3(b) for each plateau of E_{fr} .

Furthermore, we show the behavior of the weak filling fraction in the entire $\Omega_s - \Delta_s$ plane in Fig. 3(c,d). Note, that contrary to ρ_s [shown as contours in Fig. 3(a)], ρ_w exhibits a lobe like structure which is not symmetric. This can be understood as follows: For a given finite Ω_s the filling fraction ρ_s decreases with decreasing Δ_s . The resulting smaller number of s -atoms permits the accommodation of a larger number of w -atoms. This effect is stronger the larger Ω_s leading to an increasing asymmetry of the lobes in Figs. 3(c,d). Moreover, for any Δ_s , ρ_w decreases stepwise with increasing Ω_s and eventually vanishes. The decrease in ρ_w can be qualitatively explained as follows: As Ω_s increases the ground state begins to contain basis states with s -atom numbers that are larger than in the classical case. This forces the w -atoms to assume a lower filling fraction. The fraction of admixed basis states with increased s -atom number becomes larger the larger Δ_s [see contours in Fig. 3(a)] which results in the asymmetry of the lobes in Figs. 3(c,d).

We expect the qualitative features, namely the increase of frustration with Ω_s to hold also in the thermodynamic limit. To study this a semi-analytical treatment of quantum fluctuations based on a perturbative expansion of the ground state around the classical limit could in principle be performed. This task is, however, quite involved due to the fact that the filling fraction of the weak species is in fact a function of Ω_s . Nevertheless, one can still gain analytical insight into the quantum regime by considering the description of the system in terms of an approximate Hamiltonian, as is shown in the following.

5. Rokhsar Kivelson approximation

In the following we conduct an approximate analytical study of the ground state by means of a Rokhsar-Kivelson (RK) Hamiltonian H_{RK} . This generalizes the approach used in Refs. [40, 11, 41] for characterizing the statics of a Rydberg gas. The central idea is to approximate the Hamiltonian (1) as a sum of local positive semi-definite projective Hamiltonians $H_{\text{RK}} = \sum_{k=1}^L h_k$. In this case a state $|G\rangle$ can be found which is annihilated by each of the local Hamiltonians, i.e. $h_k |G\rangle = 0$, and thus represents the ground state of H_{RK} . Under the RK approximation the ground state $|G\rangle$ is given by a superposition of classical configurations of a gas of hard-core polymers. As is shown

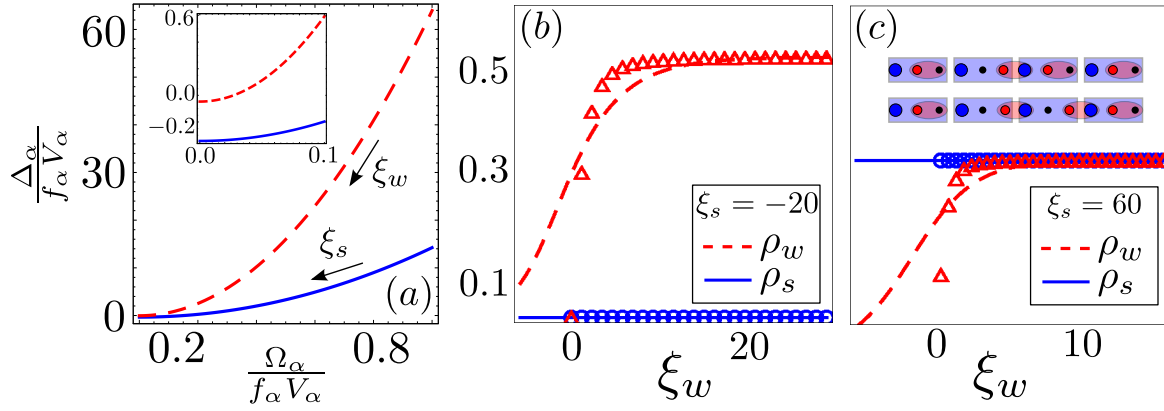


Figure 4. (Color online) (a) RK manifold of the s -atoms (solid blue line) and the w -atoms (red dashed line) for $V_s = 100V_w = 100$. The RK manifold is parameterized by the parameters ξ_α which increase when going from right to left along the manifolds. The inset show a magnification of the main figure in the region of small Ω_α . (b) Filling fractions $\rho_\alpha = (1/L) \sum_{k=1}^L \langle G | n_k^{(\alpha)} | G \rangle$ as function of ξ_w in the absence of s -atoms. Here ρ_w saturates to its unfrustrated value $1/2$. The blue circles and red triangles represent the filling fractions obtained by diagonalizing exactly Hamiltonian (1) for $L=6$ with periodic boundary conditions. We chose $V_s = 100V_w = 100$, and used the definitions of $\xi_{s,w}$ to fix $\Omega_{s,w}$, and Eq. (6) to fix $\Delta_{s,w}$. (c) In the presence of s -atoms the w -atoms can only assume a maximum filling fraction $\rho_s = 1/3$ and form a frustrated state with *exponentially many* configurations. The inset shows two example configurations with filling $\rho_w = 1/3$. Here red ellipsoids (blue rectangles) sketch the dimers (trimers) of the RK construction. The blue circles and red triangles are the exact results drawn for comparison, and are obtained with the same method explained for panel (b).

below, this procedure neglects the long-range tails in the interactions. As a consequence the densities that the different species assume in the classical limit need to be adjusted by hand.

We consider a situation where in the classical limit the densities of the weak and strong species are given by $\rho_w = 1/2$ and $\rho_s = 1/3$. In this case we can think of atoms in terms of polymers extending over sites at maximal distance $R_w = 1$ (dimers) and $R_s = 2$ (trimers), respectively (see Ref. [41] for detail). The polymer analogy is equivalent to the hard-core conditions $n_k^{(w)} n_{k\pm 1}^{(w)} = 0$ and $n_k^{(s)} n_{k\pm 1}^{(s)} = n_k^{(s)} n_{k\pm 2}^{(s)} = 0$. Neglecting interactions on distances larger than $R_\alpha + 1$ and making the hard-core conditions explicit also in the laser-excitation part of the Hamiltonian [40, 41], we can rewrite Hamiltonian (1) as

$$H = \sum_{k=1, \alpha=s,w}^L \left\{ -\Omega_\alpha \xi_\alpha + \Omega_\alpha h_k^{(\alpha)} + [\Delta_\alpha - \Omega_\alpha \xi_\alpha^{-1} - \Omega_\alpha (2R_\alpha + 1) \xi_\alpha] n_k^{(\alpha)} + \left[\frac{V_\alpha}{(R_\alpha + 1)^6} - \Omega_\alpha \xi_\alpha R_\alpha \right] n_k^{(\alpha)} n_{k+R_\alpha+1}^{(\alpha)} \right\}. \quad (4)$$

where the local Hamiltonians $h_k^{(\alpha)}$ are given by

$$h_k^{(\alpha)} = \Pi_k^{(\alpha)} \left(\sigma_k^{x(\alpha)} + \xi_\alpha n_k^{(g)} + \xi_\alpha^{-1} n_k^{(\alpha)} \right). \quad (5)$$

The $h_k^{(\alpha)}$ are the above-mentioned positive semi-definite operators which are proportional to projection operators and whose sum yields the RK Hamiltonian. The projection operators $\Pi_k^{(\alpha)}$ implement the hard-core condition by ensuring that dimers (trimers) do not occupy neighboring (next-neighboring) sites: $\Pi_k^{(w)} = p_{k-1}^{(w)} p_{k+1}^{(w)}$ and $\Pi_k^{(s)} = p_{k-2}^{(s)} p_{k-1}^{(s)} p_{k+1}^{(s)} p_{k+2}^{(s)}$ with $p_k^{(\alpha)} = 1 - n_k^{(\alpha)}$.

Hamiltonian (4) is not yet of RK form since there are a number of additional terms. For specific parameter choices, however, these terms vanish up to trivial constants. In order to make this more transparent we have introduced (following Ref. [40]) the parameters ξ_α . Those can be chosen freely since the Hamiltonian does not depend on them, as can be seen when multiplying out all the individual terms.

The RK form is assumed when choosing $\xi_\alpha = f_\alpha V_\alpha / \Omega_\alpha$ with $f_s = 1/(2 \times 3^6)$ and $f_w = 1/2^6$ and requiring the parameters $\Omega_\alpha, \Delta_\alpha, V_\alpha$ to accomplish

$$\left(\frac{\Omega_\alpha}{f_\alpha V_\alpha} \right)^2 = \frac{\Delta_\alpha}{f_\alpha V_\alpha} + g_\alpha, \quad (6)$$

where $g_s = 5$ and $g_w = 3$. The first condition eliminates the two terms in the second line of Eq. (4) while the second one leads to a cancellation of the terms proportional to Δ_α and Ω_α . Both conditions define the so-called RK-manifold [see Fig. 4(a)] on which Hamiltonian (4) assumes the RK form

$$H_{\text{RK}} = -(\Omega_s \xi_s + \Omega_w \xi_w) L + \sum_{k=1, \alpha=s,w}^L \Omega_\alpha h_k^{(\alpha)}. \quad (7)$$

The ground state $|G\rangle$ of H_{RK} is written as

$$|G\rangle = \prod_{k=1}^N \left(1 - \xi_d \Pi_k^{(w)} c_k^{(w)\dagger} - \xi_t \Pi_k^{(s)} c_k^{(s)\dagger} \right) |0\rangle, \quad (8)$$

where $|0\rangle = \bigotimes_{i=1}^N |g\rangle_i$ and $c^{(\alpha)\dagger} = |\alpha\rangle \langle g|$. The parameters ξ_α can be then thought of as the fugacities of the dimers and trimers gases, such that large (small) values result in a ground state with high (low) density of the respective species. The ground state (8) can be represented explicitly as matrix product state (see e.g. [41]). We can now use the ground state H_{RK} to get an idea of the effect of quantum fluctuations on crystalline states. We find that frustrated states emerge also away from the classical limit, i.e. for non-zero Ω_α .

By construction H_{RK} is frustration free, i.e. the frustration energy (3) is always zero. In fact this is an artifact stemming from the omission of long-range tails. Nevertheless, the interspecies frustration still manifests in the behaviour of the filling fractions, Fig. 4. In Fig. 4(b), where we set $\xi_s < 0$ in order to have a low density of dimers, we find that indeed only dimers are occupying the lattice and that they fill it completely in the limit $\xi_w \rightarrow \infty$. This corresponds to a unique (translationally invariant) crystalline ground

state with $\rho_w = 1/2$. On the other hand in Fig. 4(c) we fix the parameter ξ_s such that the strong species (trimers) fills up the lattice at density $\rho_s = 1/3$. We now increase ξ_w which increases the density of the weak species. However, instead of a saturation at density $1/2$ — as in the absence of the strong species — we find that ρ_w tends to a value of $1/3$. This is a signature of inter-species frustration. The weak species does not crystallize but is in a superposition of exponentially many states with density $1/3$, two of which are shown in the inset of Fig. 4(c).

6. Summary and outlook

We have investigated the statics of a two component Rydberg gas at zero temperature, with particular focus on the emergence of frustration effects. In the classical regime we identified regions in parameter space where the two Rydberg species form compatible and incompatible arrangements. In the quantum case we introduced the frustration energy to quantify the degree of frustration. We found that this quantity shows a staircase pattern as the system visits different phases characterized by different filling fractions. Finally, we performed an approximate analytical study of the quantum regime by means of an RK Hamiltonian, which further corroborated the existence of frustrated states.

Our analysis provides insights into the complexity of ground state structures in multi-component Rydberg gases. In the future it would be interesting to extend the work to situations without the strong-weak hierarchy that was assumed here. Moreover, an extension of the analysis to Rydberg gases with more than two relevant excited states and/or to high-dimensional lattices would be desirable due to the number of Rydberg lattice experiments that recently has become available.

7. Acknowledgements

We are very indebted to Weibin Li for providing us with data used to plot Fig. 2. E.L. would like to thank M. Marcuzzi for insightful discussions. J. M. would like to thank H. Weimer for useful discussions. The research leading to these results has received funding from the European Research Council under the European Union's Seventh Framework Programme (FP/2007-2013) / ERC Grant Agreement No. 335266 (ESCQUMA), the EU-FET grants HAIRS 612862 and from the University of Nottingham. Further funding was received through the H2020-FETPROACT-2014 Grant No. 640378 (RYSQ) and the EPSRC Grant no. EP/M014266/1.

- [1] Carr C, Ritter R, Wade C G, Adams C S and Weatherill K J 2013 *Phys. Rev. Lett.* **111** 113901
- [2] Malossi N, Valado M M, Scotto S, Huillery P, Pillet P, Ciampini D, Arimondo E and Morsch O 2014 *Phys. Rev. Lett.* **113**(2) 023006

- [3] Schempp H, Günter G, Robert-de Saint-Vincent M, Hofmann C S, Breyel D, Komnik A, Schönleber D W, Gärttner M, Evers J, Whitlock S and Weidemüller M 2014 *Phys. Rev. Lett.* **112**(1) 013002 URL <http://link.aps.org/doi/10.1103/PhysRevLett.112.013002>
- [4] van Ditzhuijzen C S E, Koenderink A F, Hernández J V, Robicheaux F, Noordam L D and van den Heuvell H B v L 2008 *Phys. Rev. Lett.* **100**(24) 243201 URL <http://link.aps.org/doi/10.1103/PhysRevLett.100.243201>
- [5] Günter G, Schempp H, Robert-de Saint-Vincent M, Gavryusev V, Helmrich S, Hofmann C S, Whitlock S and Weidemüller M 2013 *Science* **342** 954–956 ISSN 0036-8075, 1095-9203 URL <http://www.sciencemag.org/content/342/6161/954>
- [6] Barredo D, Labuhn H, Ravets S, Lahaye T, Browaeys A and Adams C S 2014 *preprint* arXiv:1408.1055
- [7] Schachenmayer J, Lesanovsky I, Micheli A and Daley A J 2010 *New Journal of Physics* **12** 103044
- [8] Pohl T, Demler E and Lukin M D 2010 *Phys. Rev. Lett.* **104** 043002
- [9] van Bijnen R M W, Smit S, van Leeuwen K A H, Vredenburg E J D and Kokkelmans S J J M F 2011 *Journal of Physics B: Atomic, Molecular and Optical Physics* **44** 184008
- [10] Sela E, Punk M and Garst M 2011 *Phys. Rev. B* **84**(8) 085434 URL <http://link.aps.org/doi/10.1103/PhysRevB.84.085434>
- [11] Lesanovsky I 2012 *Phys. Rev. Lett.* **108**(10) 105301
- [12] Ji S, Ates C and Lesanovsky I 2011 *Phys. Rev. Lett.* **107**(6) 060406 URL <http://link.aps.org/doi/10.1103/PhysRevLett.107.060406>
- [13] Höning M, Muth D, Petrosyan D and Fleischhauer M 2013 *Phys. Rev. A* **87**(2) 023401 URL <http://link.aps.org/doi/10.1103/PhysRevA.87.023401>
- [14] Weimer H and Büchler H P 2010 *Phys. Rev. Lett.* **105**(23) 230403
- [15] Vermersch B, Punk M, Glaetzle A W, Gross C and Zoller P 2015 *New Journal of Physics* **17** 013008 URL <http://stacks.iop.org/1367-2630/17/i=1/a=013008>
- [16] Schauf P, Zeiher J, Fukuhara T, Hild S, Cheneau M, Macrì T, Pohl T, Bloch I and Gross C 2014 *Science* **347** 1455–1458
- [17] Li W, Viscor D, Hofferberth S and Lesanovsky I 2014 *Phys. Rev. Lett.* **112**(24) 243601 URL <http://link.aps.org/doi/10.1103/PhysRevLett.112.243601>
- [18] Bettelli S, Maxwell D, Fernholz T, Adams C S, Lesanovsky I and Ates C 2013 *Phys. Rev. A* **88**(4) 043436 URL <http://link.aps.org/doi/10.1103/PhysRevA.88.043436>
- [19] Maxwell D, Szwer D J, Paredes-Barato D, Busche H, Pritchard J D, Gauguier A, Jones M P A and Adams C S 2014 *Phys. Rev. A* **89**(4) 043827 URL <http://link.aps.org/doi/10.1103/PhysRevA.89.043827>
- [20] Saffman M, Walker T G and Mølmer K 2010 *Rev. Mod. Phys.* **82** 2313
- [21] Béguin L, Vernier A, Chicireanu R, Lahaye T and Browaeys A 2013 *Phys. Rev. Lett.* **110**(26) 263201 URL <http://link.aps.org/doi/10.1103/PhysRevLett.110.263201>
- [22] Gorniaczyk H, Tresp C, Schmidt J, Fedder H and Hofferberth S 2014 *Phys. Rev. Lett.* **113**(5) 053601 URL <http://link.aps.org/doi/10.1103/PhysRevLett.113.053601>
- [23] Tiarks D, Baur S, Schneider K, Dürr S and Rempe G 2014 *Phys. Rev. Lett.* **113**(5) 053602 URL <http://link.aps.org/doi/10.1103/PhysRevLett.113.053602>
- [24] Wu F Y 1982 *Rev. Mod. Phys.* **54** 235
- [25] Herrmann H J and Martín H O 1984 *J. Phys. A* **17** 657
- [26] Glumac Z and Uzelac K 1993 *J. Phys. A* **26** 5267
- [27] Cannas S A and de Magalhães A C N 1997 *J. Phys. A* **30** 3345
- [28] Bayong E, Diep H T and Dotsenko V 1999 *Phys. Rev. Lett.* **83** 14
- [29] Hubbard J 1978 *Phys. Rev. B* **17**(2) 494–505 URL <http://link.aps.org/doi/10.1103/PhysRevB.17.494>
- [30] Gallagher T F 1994 *Rydberg Atoms* (Cambridge University Press, Cambridge)
- [31] Löw R, Weimer H, Nipper J, Balewski J B, Butscher B, Büchler H P and Pfau T 2012 *J. Phys. B: At. Mol. Opt. Phys.* **45** 113001

- [32] Olmos B, Li W, Hofferberth S and Lesanovsky I 2011 *Phys. Rev. A* **84**(4) 041607 URL <http://link.aps.org/doi/10.1103/PhysRevA.84.041607>
- [33] Celistrino Teixeira R, Hermann-Avigliano C, Nguyen T L, Cantat-Moltrecht T, Raimond J M, Haroche S, Gleyzes S and Brune M 2015 *ArXiv e-prints (Preprint 1502.04179)*
- [34] Singer K, Stanojevic J, Weidemüller M and Côté R 2005 *J. Phys. B* **38** S295
- [35] Pokrovsky V L and Uimin G V 1978 *Journal of Physics C: Solid State Physics* **11** 3535 URL <http://stacks.iop.org/0022-3719/11/i=16/a=022>
- [36] Bak P and Bruinsma R 1982 *Phys. Rev. Lett.* **49**(4) 249–251 URL <http://link.aps.org/doi/10.1103/PhysRevLett.49.249>
- [37] Burnell F J, Parish M M, Cooper N R and Sondhi S L 2009 *Phys. Rev. B* **80**(17) 174519 URL <http://link.aps.org/doi/10.1103/PhysRevB.80.174519>
- [38] Levi E, Minář J and Lesanovsky I 2015 *ArXiv e-prints (Preprint 1503.03268)*
- [39] Schauf P, Cheneau M, Endres M, Fukuhara T, Hild S, Omran A, Pohl T, Gross C, Kuhr S and Bloch I 2012 *Nature* **491** 87–91 ISSN 0028-0836 URL <http://www.nature.com/nature/journal/v491/n7422/full/nature11596.html>
- [40] Lesanovsky I 2011 *Phys. Rev. Lett.* **106**(2) 025301
- [41] Levi E and Lesanovsky I 2014 *New Journal of Physics* **16** 093053 URL <http://stacks.iop.org/1367-2630/16/i=9/a=093053>